# 24

# Microscopic Analysis of Fluorescence Resonance Energy Transfer (FRET)

**Brian Herman, R. Venkata Krishnan, and Victoria E. Centonze**


## Abstract

We describe here detailed practical procedures for implementing various approaches of fluorescence resonance energy transfer (FRET) in microscope-based measurements. A comprehensive theoretical formalism is developed and the different experimental procedures are outlined. A step-by-step protocol is provided for preparing the specimens for FRET measurements, data acquisition procedures, analysis, and quantification. Particular emphasis is given to exemplify the FRET applications in the study of protein–protein interactions.



## Key Words

Microscopy; FRET; FLIM; protein interactions.


## 1. Introduction

The ability to spatially resolve ever-smaller structures defines any advancement in microscopy. Resolution is defined as the smallest distance between any two points (or structures) so as to be able to distinguish them clearly in space, the numerical estimate of which is given by Rayleigh's criterion:

$$d = 0.6\lambda/\mathrm{NA} \quad (1)$$

As can be seen, spatial resolution (or the minimum resolving distance, $d$) varies directly with the wavelength ($\lambda$) of the light used and inversely with the numerical aperture (NA) of the objective lens used. Although electron microscopes can offer greater resolution than optical imaging using visible wavelengths of light, this form of microscopy is not useful for live cell applications because of the non-native imaging environment (vacuum) and other stringent specimen preparation conditions that are required. Additionally, one cannot

From: *Methods in Molecular Biology, vol. 261: Protein–Protein Interactions: Methods and Protocols*
Edited by: H. Fu © Humana Press Inc., Totowa, NJ

increase NA indefinitely as this would lead to impractically small working distances between the specimen and the objective. Thus, biological imaging applications are limited to visible light and maximal NA of approx 1.5–1.6. Considering these limitations, the best possible resolution achievable by any light microscope is approx 250 nm. Modern confocal and multiphoton microscopes do have improved axial resolution compared to their wide-field counterparts; however, they still suffer the same limitations of lateral resolution *(1)*. Although there have been some recent developments that have increased the spatial resolution of the optical microscope beyond this limit, no optical microscope allows observations of objects at the molecular level *(2)*. This limitation has made it difficult to study a number of physiological and metabolic processes in cells that result from interaction between macromolecules on a spatial scale of a few nanometers. Fluorescence (Forster) resonance energy transfer (FRET) holds an unique niche in modern fluorescence microscopy because it provides the means by which one can probe inter- and intra-molecular interactions in the 1–10 nm range *(3–6)*. FRET microscopy methods do not improve the resolution *per se* over that of conventional light microscopy methods but only extend the detection limit to a few nanometers. In other words, FRET microscopy yields quantitative information about the molecular interactions occurring in the range of 1–10 nm that is otherwise impossible to obtain using other light microscopy methods. For a biologist, this implies that it is possible to extend light microscopy from being a mere visualization tool to a precise quantitative tool—while addressing the various issues of macromolecular interactions on a molecular level. This chapter attempts to provide the novice in this field with practical notes for implementing the different FRET approaches for cell biological applications.

### 1.1. Theoretical Formalism

Quantum mechanically, there exists a certain probability that an excited donor can transfer a part of its excitation energy nonradiatively to a neighboring molecule (via direct dipole–dipole interactions) in addition to other classical radiative decay processes *(7)*. These two decay paths differ in their time scales: radiative fluorescence decay occurs typically over a few nanoseconds after excitation, whereas the nonradiative energy transfer process is 100–1000 times faster than the radiative decay. FRET is one such nonradiative decay process and requires stringent conditions in terms of the spatial as well as spectral relationship between the donor and acceptor (*see* **Note 1**). Energy transfer efficiency ($E$) serves as a quantitative measure of the FRET process. It is therefore natural that all the available experimental approaches are designed to measure $E$ in various circumstances. The energy transfer efficiency depends on the relative orientation and separation ($R$) between the donor and acceptor dipoles

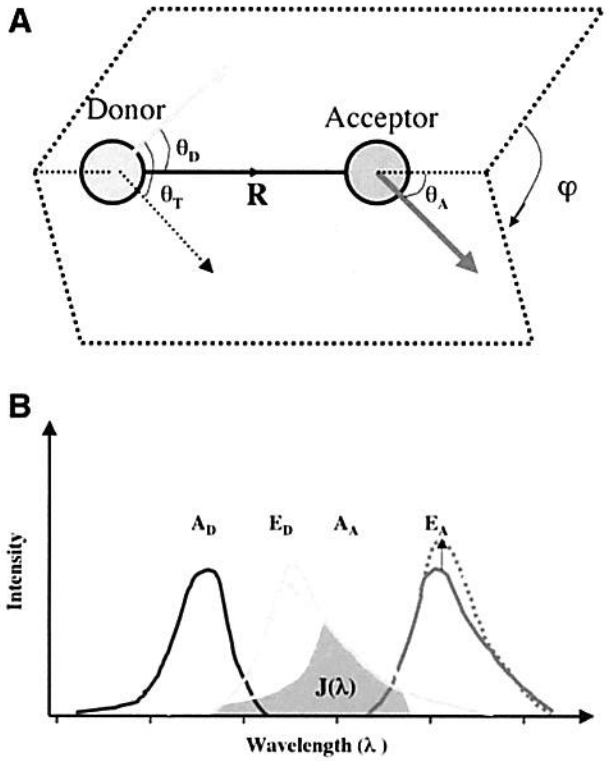


Fig. 1. **(A)** A schematic representation of FRET mechanism. The angles and distance of separation are explained in **Note 1**. **(B)** Schematic of energy transfer in terms of donor/acceptor spectra.

(**Fig. 1A**) in addition to the overlap between the donor emission and the acceptor absorption spectra (**Fig. 1B**). This relationship is given by

$$E = \frac{R_0^6}{R_0^6 + R^6} \tag{2}$$

By definition, $R_0$ ("Forster distance") is the distance of separation at which the energy transfer efficiency is 50%, that is to say, when $R = R_0$ there exist equal probabilities that nonradiative energy transfer and radiative deactivation can occur from the donor excited state. See **Note 1** for a detailed explanation of individual parameters in the above Forster equation. What gives the FRET phenomenon its sensitivity and specificity is the sixth-power dependence of transfer efficiency on the distance separating the donor–acceptor (*see* **Note 2**).

Because the likelihood of energy transfer varies by the sixth power of the distance between the donor and acceptor, even very small (angstrom level) separations can be measured reliably. In practice, this provides the effectiveness of the FRET measurement in the range 1–10 nm and effectively extends the measurement resolution of the fluorescent microscope beyond that of conventional light microscopy. Because the measurement of $E$ and a few other constants (*see* **Note 1**) can yield an estimate of distance of separation between the pair of fluorescent molecules that undergo energy transfer, FRET process is often referred to as "spectroscopic ruler" *(8)*. The phenomenon of energy transfer also contains molecular information which is different from that revealed by solvent-relaxation, fluorescence quenching, and so on, which provide information about the interaction of the fluorophore with the neighboring molecules in the surrounding solvent shell *(7)*. There are various manifestations of the FRET process, and the following section gives a brief account of the different approaches that can be adopted to measure the energy transfer efficiency.

### 1.2. FRET Experimental Approaches

#### 1.2.1. Donor Quenching/Sensitized Emission of the Acceptor Fluorescence

Because the donor emission fluorescence is quenched upon energy transfer, the ratio of donor emission fluorescence to the acceptor emission fluorescence intensity can be used as a good measure of the energy transfer efficiency (**Fig. 1B**). It is possible to quantify these ratios in individual cells. The most conventional form of observing the energy transfer event is to excite the donor and observe the fluorescence from both the donor and acceptor *(3)*. The transfer efficiency in this case can be expressed as

$$E = 1 - \left(I_{DA}/I_{D}\right) \tag{3}$$

where $I_{DA}$ is the donor fluorescence in the presence of acceptor (energy transfer condition) and $I_{D}$ is the donor fluorescence when there is no energy transfer. This method can be implemented in both wide-field and confocal microscopes (*see* **Fig 2** and **Note 3**).

#### 1.2.2. Donor Dequenching Upon Acceptor Photobleaching

If the acceptor molecules are sufficiently photolabile, then another way of monitoring FRET is to observe the increase (or the recovery) in donor fluorescence when the acceptors are selectively photobleached. Energy transfer efficiency can be now calculated from the following equation:

$$E = 1 - \left(I_{D(pre)}/I_{D(post)}\right) \tag{4}$$

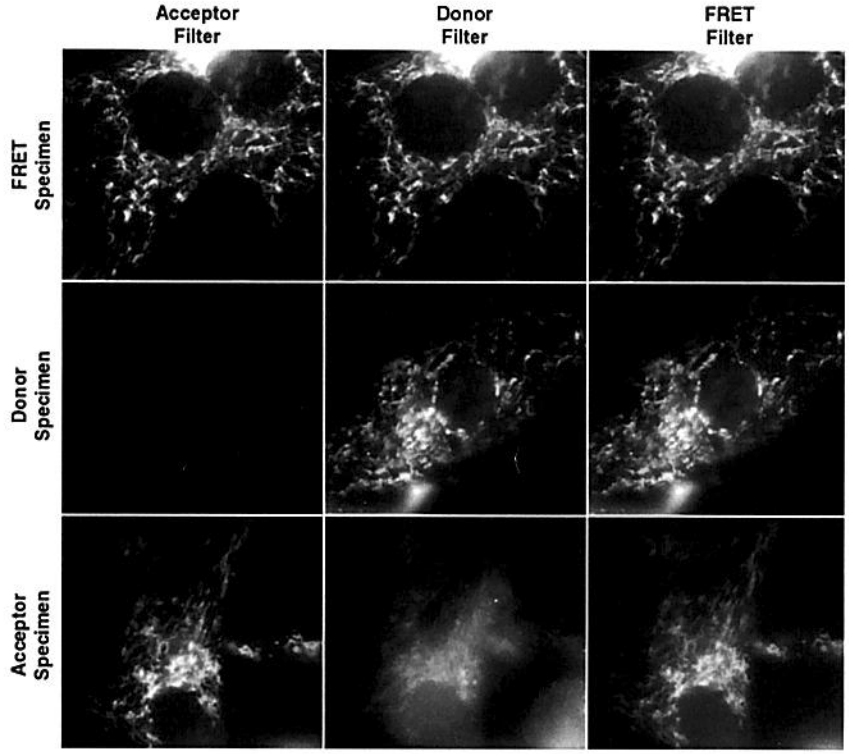


Fig. 2. FRET measurement by sensitized emission approach. The nine-panel image shows donor-only, acceptor-only, and FRET specimens taken with the three different filter sets marked in the figure. Baby hamster kidney (BHK) cells were transfected with mitochondrially targeted protein constructs: **(A)** mCFP: *Donor only*; **(B)** mYFP: *Acceptor only*; and **(C)** mCGY: *FRET specimen*. The measurements were carried out in Olympus IX-70 inverted microscope with appropriate excitation and emission filters as described in **Table 1**. The data acquisition and analysis are carried out as described in **Subheading 3.3.**

where $I_{D(pre)}$ and $I_{D(post)}$ are the donor intensities in pre- and postbleaching conditions. An advantage of this method is that one can use laser scanning confocal or multiphoton microscopy to visualize even small regions in cells and to selectively photobleach the acceptor in these small regions. In this way, one can achieve a high spatial resolution in the FRET measurement. Jovin and Jovin have introduced an alternate way of obtaining energy transfer efficiency by photobleaching the donor instead of the acceptor *(9)*.

Photobleaching depletes the excited state of donor population and this leads to an inverse relationship between the photobleaching time constant and the fluorescence lifetime of the donor. The FRET process results in a decrease in the donor lifetime and hence a corresponding increase in the photobleaching time constant. Energy transfer efficiency can be calculated by measuring this bleaching time constant for the donor in the presence and absence of acceptors. However, as many biological experiments require keeping cells alive under long periods of observation, the use of either acceptor or donor photobleaching approaches can result in irreversible photobleaching of the cells (*see* **Fig. 3** and **Note 4**).

### *1.2.3. Concentration-Dependent Depolarization of Fluorescence*

The transition dipoles of most fluorophores are anisotropic. When excited with plane-polarized light, their emission also becomes plane polarized. Rotational diffusion of the fluorophores during the excited-state lifetime is generally found to be the dominant cause of depolarization *(7)*. Depending on the relative magnitudes of the rotational diffusion time ($\phi$) and the intrinsic lifetime ($\tau$) of the fluorophore, the change in anisotropy ($r$) of a fluorophore can be calculated by the Perrin equation *(7)*:

$$r = \frac{r_0}{1 + (\tau / \phi)} \tag{5}$$

where $r_0$ (=2/5 ) is the limiting anisotropy for a randomized ensemble of fluorophores and using single-photon excitation. One of the consequences of FRET is that, if the donor is excited with plane-polarized light, then following an energy transfer event, the acceptor fluorescence is depolarized. The corresponding energy transfer efficiency can be calculated by the following equation ***(10)***:

$$E = 1 - (r / r^0) \tag{6}$$

where $r$ and $r^0$ are the measured anisotropies of the acceptor with and without energy transfer, respectively. An advantage of this method is that one can use this to measure homo-FRET (i.e., where the same fluorophore serves as both donor and acceptor) when the fluorophore used has a sufficient overlap between its own excitation and emission spectra (i.e., very small Stokes' shift) (***11–14***; *see* **Note 5**).

### *1.2.4. FLIM : Reduction of Donor Lifetime Upon Energy Transfer*

Another important manifestation of a FRET event is that the donor lifetime decreases upon the energy transfer *(7)*. This can be exploited experimentally by measuring the fluorescence lifetime of the donor in the presence and absence of the acceptor by one of the many time-domain or frequency-

**Table 1**
**Typical FRET Pairs and the Corresponding Filter Combinations[a]**

| | Donor imaging path | | | Acceptor imaging path | | |
|---|---|---|---|---|---|---|
| FRET Pair | Excitation filter | Dichroic | Emission filter | Excitation filter | Dichoric | Emission filter |
| FITC–TRITC | 480/40 | 505 LP | 535/40 | 545/30 | 565 LP | 610/60 |
| FITC–Cy3 | 480/40 | 505 LP | 535/40 | 540/25 | 565 LP | 605/55 |
| Cy3–Cy5 | 540/25 | 565 LP | 605/55 | 640/20 | 660 LP | 680/30 |
| BFP–GFP | 390/20 | 420 LP | 460/50 | 475/40 | 460 LP | 535/50 |
| GFP–Cy3 | 475/40 | 460 LP | 505/40 | 540/25 | 565 LP | 605/55 |
| CFP–YFP | 436/20 | 455 LP | 480/40 | 500/20 | 515 LP | 535/30 |
| CFP–DsRed | 436/20 | 455 LP | 480/40 | 546/12 | 560 LP | 620/20 |

[a] All the values are expressed as center wavelength (nm) with the spread on either side of the peak value. Donor-only and acceptor-only images are acquired separately with donor and acceptor filter sets, respectively. FRET images are acquired with donor excitation filter, donor dichroic and acceptor emission filter. These filter combinations were adapted from the catalog of filter sets published by Chroma Techonology Corporation.

domain fluorescence lifetime imaging microscopy (FLIM) methods ***(15–17)***. The energy transfer efficiency can be calculated by

$$E = 1 - \left(\tau_{DA}/\tau_{D}\right) \tag{7}$$

where $\tau_{DA}$ and $\tau_{D}$ are the donor lifetimes in the presence and absence of acceptor. The main advantage of this technique is that the FRET signal depends only on the excited-state reactions and not on the donor concentration or light path length. Furthermore, this method does not suffer from problems due to cross-talk between the donor and acceptor spectra or the need to precisely control the concentration of the donor and acceptor (*see* **Note 6**).

In the following sections, we give a generalized outline of equipments and procedures for implementing the various FRET approaches described above. As the field of FRET microscopy is rapidly progressing in a variety of applications, it is not possible to cover all these specific details in this chapter. It is therefore recommended to take care of the specific requirements (besides the general guidelines given below) for cell culture and handling before implementing the FRET measurements. For the sake of exemplification, we choose a specific FRET pair, namely, cyan fluorescent protein–yellow fluorescent protein (CFP-YFP) and typical equipments that we use routinely in our laboratory. However, the general theme of **Materials** and **Methods** holds good for any combination of FRET pairs and is valid for all the different FRET approaches described in this section.

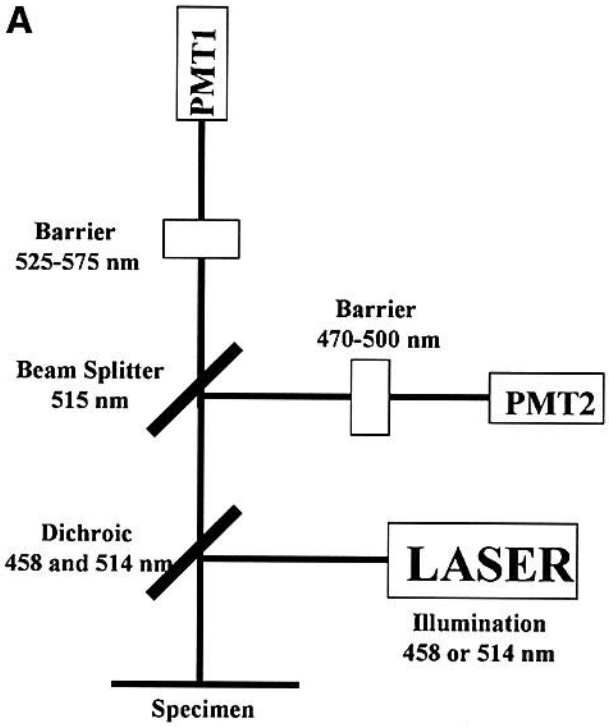


Fig. 3. **(A)** Typical imaging path in the laser scanning confocal microscope for the specific FRET pair CFP-YFP. Laser excitation (458 nm for CFP and 514 nm for YFP) from the source is routed through the dichroic to the specimen. The fluorescence emission from the specimen passes through the dichroic to the beam splitter. Fluorescence signal below 515 nm is reflected toward the CFP emission filter (470–500 nm bandpass) and detected by the photomultiplier tube (PMT2) in the donor (CFP) channel. The rest of the signal (>515 nm) passes through the beam splitter and the YFP emission filter (525–575 nm bandpass) and eventually gets recorded in the acceptor (YFP) channel. For FRET imaging, the specimen is excited with donor excitation wavelength (458 nm) and the signal is detected in the acceptor channel. **(B)** FRET measurement by Acceptor photobleaching approach. The FRET sample (mCGY) sample is the same as in **Fig.2**. The measurements were carried out in Zeiss-LSM510 confocal microscope with 458 nm and 514 nm laser lines for exciting CFP and YFP, respectively. HT515LP dichroic was used in the excitation path and the fluorescence emission from CFP and YFP were collected through the bandpass filters 470-500 nm and 525–575 nm respectively. The data acquisition and analysis are carried out as described in **Subheading 3.3.** The upper panel shows the images of the FRET sample in donor- and acceptor-channels—both before and after photobleaching by 514 nm laser line. Many regions were marked in the mitochondria and an average of fluorescence intensity in these regions is calculated and is given in the lower panel of the figure; 20% FRET efficiency was obtained in these conditions as calculated.

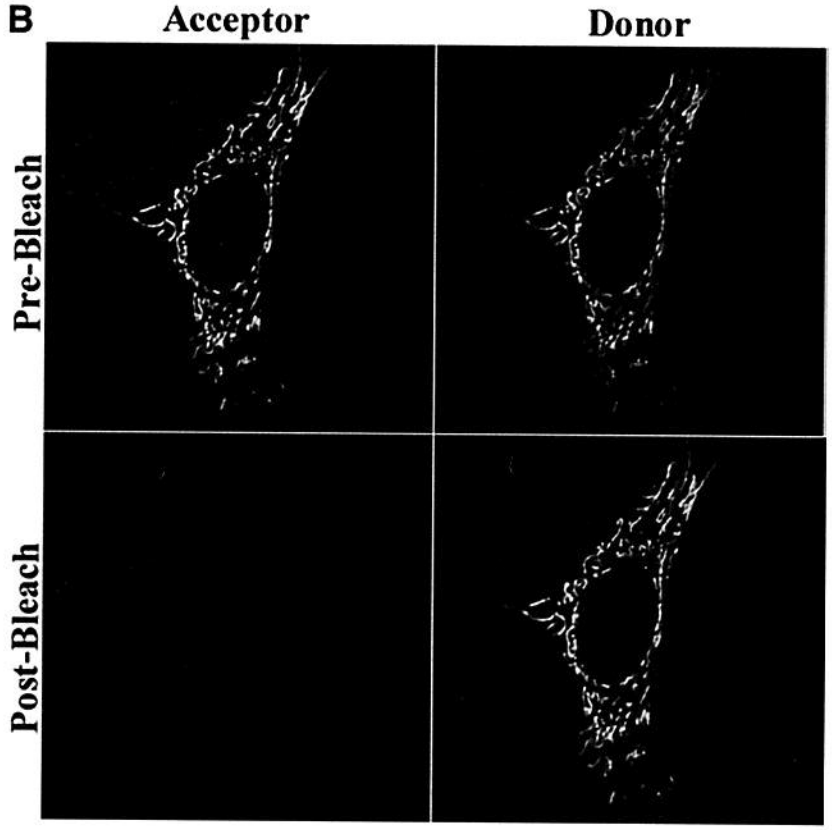
B
Acceptor
Donor
Pre-Bleach
Post-Bleach

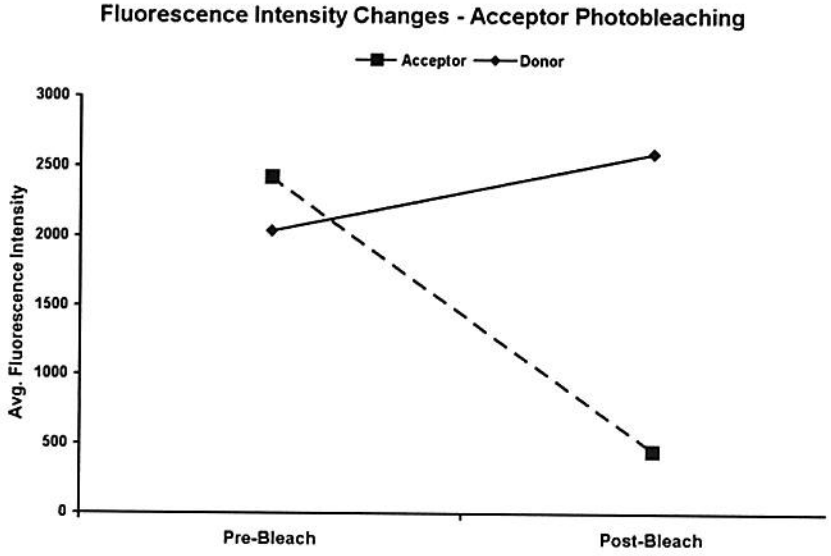
Fluorescence Intensity Changes - Acceptor Photobleaching
Acceptor
Donor
Avg. Fluorescence Intensity
3000
2500
2000
1500
1000
500
0
Pre-Bleach
Post-Bleach

## 2. Materials

### 2.1. Optics and Illumination

1. *Wide-field system*: A research grade microscope, with high NA optics that are corrected for spherical and chromatic aberrations. The microscope must be equipped with an epi-fluorescence attachment and a high-intensity light source (e.g. Olympus IX-70 microscope equipped with 60X PlanApo lens and mercury arc source).
2. *Scanning confocal system*: Confocal laser scanning imaging system with lasers appropriate for excitation of the chosen donor/acceptor FRET pairs, e.g., a Zeiss 510 laser scanning confocal microscope equipped with an argon ion laser emitting lines of 458 nm, 488 nm, and 514 nm for excitation of CFP, GFP, and YFP, respectively, green HeNe emitting at 543 nm for excitation of DsRed, rhodamine, and Cy3, and a red HeNe emitting at 633 nm for excitation of Cy5 and allophycocyanine.

### 2.2. Filters

1. *Wide-field system*: Excitation/emission filters for appropriate excitation/emission wavelength selection for the donor/acceptor to be employed (**Table 1**). Excitation and emission filters may be placed in cubes along with the dichroic filters. Alternatively, the excitation and emission filters may be placed in filter wheels for automated, rapid switching (*see* **Note 7**).
2. *Scanning confocal system*: The confocal system should have beamsplitters and emission filters in place such that specific pathways can be configured for acquisition of the acceptor signal only, the donor signal only, and the FRET signal. Acquisition of the FRET signal should be done by illuminating with the donor excitation wavelength but collecting the acceptor emission (*see* **Fig. 3A** for typical configuration). It is recommended to employ sequential imaging mode to acquire signal from each imaging pathway independently. By taking images in sequence rather than simultaneously, the bleed-through or cross-talk between filters is significantly reduced.

### 2.3. Detectors

The key features for choosing the right digital camera are high quantum efficiency over the entire visible spectrum of wavelengths, large dynamic range, low read noise, and minimum dark current. (*see* **Note 8**) It is useful to have a digital camera system with sufficient bit depth to be able to resolve very slight changes in fluorescence intensities. Charge-coupled device (CCD) cameras such as Hamamatsu Orca cameras are recommended. For FLIM imaging, it is imperative to use fast cameras coupled to microchannel plate photomultiplier tubes with very fast rise times (approx 0.3 ns).

### 2.4. Data Acquisition and Analysis

Image acquisition and analysis in fluorescence microscopy are now largely integrated in a few commercially available software systems. The essential

**Table 2**
**Representative Websites of the Manufacturers[a]**

| | |
|---|---|
| Optics and Illumination | 1. Coherent Inc.: http://www.coherent.com<br>2. Spectra-Physics: http://www.spectraphysics.com<br>3. Perkin Elmer: http://optoelectronics.perkinelmer.com<br>4. Hamamatsu Photonics: http://www.hamamatsu.com<br>5. Nikon Instruments Inc: http://www.nikon.com<br>6. Olympus America: http:// www.olympus.com<br>7. Carl Zeiss Microimaging: http:// www.zeiss.com<br>8. Melles-Griot: http:// www.mellesgriot.com/<br>9. NewPort Corp.:http:// www.newport.com |
| Filters | 1. Omega Optical: http:// www.omegafilters.com<br>2. Chroma Technology Corp.: http://www.chroma.com |
| Detectors | 1. Hamamatsu Photonics: http://www.hamamatsu.com<br>2. Jobin Yvon: http:// www.jyhoriba.com<br>3. Perkin Elmer: http://optoelectronics.perkinelmer.com |
| Data acquisition | 1. Universal Imaging Corp.: http://www.universal-imaging.com<br>2. Q Imaging: http://www.qimaging.com<br>3. Intelligent Imaging Innovations: http://www.intelligent-imaging.com<br>4. BioRad Laboratories: http://www.micoroscopy.bio-rad.com |
| Fluorophores | 1. BD Biosciences Clontech: http:// www.clontech.com<br>2. Molecular Probes Inc.: http:// www.probes.com |

[a] A partial list of manufacturers dealing with equipment needed for implementing FRET approaches in microsocope based systems.

requirement from any analysis package is that it should be able to select defined regions of interest and to measure the same regions between different images, for example, between acceptor/donor/FRET images in the case of sensitized emission or between pre- and postbleach images in the case of acceptor photobleaching approach. The measured intensities can then be transferred to spreadsheets for calculation of FRET efficiency. In our laboratory, journals have been written in MetaMorph (Universal Imaging Corp.) for both acquiring images as well as for further analysis to calculate normalized FRET (FRETN). Similar software packages are also available from other sources *(18)*. **Table 2** gives a comprehensive list of manufacturers and useful websites pertinent to fluorescence imaging and FRET microscopy.

### 2.5. Fluorophores

**Table 1** summarizes a list of commonly used FRET pairs for studying protein–protein interactions. The choice of FRET pair depends on the spectral characteristics of donor and acceptor fluorophores. Regardless of the approach employed to measure FRET, these conditions remain the same (*see* **Note 1**). A vital advancement in the armamentarium of fluorophores for microscopy came with the discovery of green fluorescent protein (GFP) and its various spectral mutants *(19,20)*. As these fluorescent proteins can be fused to the protein of one's interest within a living cell, FRET applications can include intracellular imaging and dynamic tracking of interactions between these proteins.

### 2.6. Reagents

1. PHEM: 60 m*M* PIPES, 25 m*M* HEPES, 10 m*M* EGTA, 2 m*M* $MgCl_2$.
2. Plasmid Mini-Prep Kit (Qiagen, Chatworth, CA).
3. DNA transfection reagent: Fugene (Roche).
4. Formaldehyde solution: 4% paraformaldehyde, pH 7.2–7.4, in PHEM buffer.
5. $NaBH_4$ (1 mg/mL).
6. Mounting medium: Vectashield (Vector) or Mowiol (Polysciences, Inc.) containing 1 mg/mL para-phenylene diamine.

## 3. Methods

### 3.1. Construct Preparation

1. In our laboratory, we employ mitochondrially targeted fluorescent proteins such as mCFP, mYFP, and mCGY (fusion protein of CFP and YFP linked through a polyglycine linker).
2. DNA transformation is carried out in bacterial cell cultures.
3. DNA is isolated using a Plasmid Mini-Prep Kit. DNA sequence for each vector is verified by an independent DNA sequencing laboratory. Glycerol stocks are made of transformed cells for future experiments.

### 3.2. Specimen Preparation

#### 3.2.1. Cell Culture/Transfection

1. No. 1.5 glass coverslips are sterilized by alcohol wash and flaming or by autoclaving. Cells are then cultured on these coverslips in the preferred medium and at the appropriate temperature/atmosphere.
2. At approx 30–50% confluence, purified DNA is introduced into baby hamster kidney (BHK) cells with Fugene according to the instructions provided by the manufacturer. Typically, 2 μg DNA is mixed with 6 μL Fugene reagent in 100 μL serum-free OptiMem medium and incubated at room temperature for 45 min before adding to the cells.
3. After the transfection period, cells are rinsed and fresh medium is added to the cultures. Fluorescent proteins may be observed in cells between 6 and 24 h post-

transfection. At this time live cells may be transferred to a viewing chamber to measure FRET in the living cells. If cells are imaged live, it is recommended that a HEPES-buffered medium without phenol red be used instead of the conventional medium. Temperature should be maintained at 37°C using a heater stage. Alternatively, the cells may be fixed and mounted (approx 16–24 h post-transfection) for future use.

#### 3.2.2. Fixation and Mounting of Cells for FRET Measurements

1. Medium is rinsed from transfected cells using PHEM or other appropriate buffer (*see* **Note 9** for situations that do not involve transfection but antibody labeling).
2. Cells are fixed for 20 min at room temperature with freshly prepared 4% paraformaldehyde, pH 7.2–7.4, in PHEM buffer.
3. After fixation, cells are rinsed twice with buffer.
4. Cells are incubated with 1 mg/mL $NaBH_4$, three changes for 5 min each. This step suppresses cellular autofluorescence significantly.
5. Cells are rinsed with buffer and mounted in Vectashield (Vector) or Mowiol (Polysciences, Inc.) containing 1 mg/mL para-phenylene diamine.
6. Excess mounting medium is removed and the coverslips are sealed with epoxy or nail hardener (*see* **Note 10**).
7. For extended use of fixed specimens, it is important that the slides are kept in dark and at 4°C.

### 3.3. Data Acquisition

#### 3.3.1. Sensitized Emission FRET1

1. For detection of sensitized emission FRET, it is recommended that a three-sample/three-filter set approach be employed as detailed in Gordon et al. *(21)*. As stated previously, most sensitized emission measurements with filter-based microscopes suffer from problems of filter cross-talk or bleed through. The three-filter set method is the most conservative and the most general approach to the calculation FRETN that corrects for this cross-talk, and can be implemented on any microscope or microfluorimeter. For each measurement of FRET, three samples must be prepared—one containing donor-only (d), one containing acceptor-only (a), and one that contains both donor and acceptor (f). Each of the samples is imaged with an acceptor filter set (A), a donor filter set (D), and a FRET filter set (F).
2. For the correction algorithms to work effectively, the FRET filter set must be configured to have an exciter and dichroic that is *matched* with the donor-only filter set and an emitter filter that is *matched* with the acceptor-only filter set. (*see* **Notes 11** and **12** and **Table 1**).
3. Acquisition settings for the filter sets are determined by imaging a representative area of the donor sample with the donor filter set, the acceptor sample with the acceptor filter set, and the FRET sample with the FRET filter set. Exposure time, light intensity, and camera settings are adjusted to acquire images with

good signal-to-noise ratio. It is reasonable to select settings that will utilize approx 60–80% of the dynamic range to allow for sample variation. Once these settings are determined, they must remain constant for the filter set or imaging pathway regardless of the sample being observed. For every specimen at least 10 fields are imaged with each of the three filters sets.

#### 3.3.2. Acceptor Photobleaching FRET

In the case of the acceptor photobleaching FRET approach, first an image of the donor fluorescence is acquired. Then the acceptor molecule is selectively photobleached by extensive illumination of the specimen with wavelengths of light centered at the absorption maximum of the acceptor. Photobleaching may be done in a wide-field microscope by continuously illuminating the sample using an acceptor-only filter set or in a confocal microscope with the laser line required for acceptor excitation—until the acceptor signal is destroyed. This may be easily performed in a confocal microscope implementing a time-lapsed bleach.

#### 3.3.3. FLIM–FRET

In the case of either of the FLIM methods, FRET measurements involve monitoring only the donor lifetime for calculation of transfer efficiency according to eq. 6. Lifetimes can be calculated for the whole cell or in some specific regions of the cell depending on the requirements. This is the only method that does not obviously depend on the acceptor concentration and light path length. However, it may be important to monitor donor lifetimes at various acceptor concentrations to optimize the sensitivity of the system to FRET.

### 3.4. Analysis and Quantification

1. Each of the different FRET approaches discussed above yields two-dimensional images and the extent of FRET signal is calculated from changes in intensities or lifetimes due to FRET either in the whole cell or in smaller regions inside the cell.
2. In the case of sensitized emission FRET approach, first, the regions of local background in each image of a stack are measured to determine the average fluorescence contribution from this source. Next, regions of interest are marked. A detailed analysis procedure of these regions of interest is given in Gordon et al. *(21)*.
3. Implementation of the three-sample/three-filter set approach and correction of the resulting FRET signals to determine FRETN results in a highly corrected value for FRET. Because this is an arbitrary number, it is very important to compare the FRETN value from a given experiment to a FRETN calculated from a negative control sample, one for which there should be little or no FRET. Whenever possible, it is also recommended that a positive control sample also be analyzed.
4. In the case of acceptor photobleaching FRET approach, donor fluorescence in regions of interest are measured from the prebleach and postbleach images. The

energy transfer efficiency is calculated according to eq. 4. It is to be noted that incomplete photobleaching (≤ 95%) of the acceptors can cause a significant error in the calculated energy transfer efficiency.

5. As mentioned earlier, energy transfer efficiency is a good quantitative measure of the FRET phenomenon. It is therefore a reliable parameter that should be monitored when comparing the FRET results for a given specimen measured by different FRET approaches described above.

By virtue of being a quantitative addendum to the conventional fluorescence methods, FRET microscopy approach allows analysis of cell component interactions in a rigorous quantitative framework. The FRET equation (eq. 2) is a nonlinear function of donor–acceptor separation and care has to be taken in interpreting small changes in intensity where many noise contributions are inevitable and may be significant (*see* **Note 13**). It is therefore critical to take into account the applicable corrections (optics/electronics) in designing a FRET experiment in the context of protein–protein interactions. Because the phenomenon of FRET is a stochastic process, failure to detect FRET in laboratory experiments does not necessarily rule out interactions among the molecules, but only sets a lower limit of sensitivity in detecting those interactions. This chapter is an attempt to set some general guidelines and protocols to enable sensitive and reliable detection of protein–protein interactions. Most of the discussions in this chapter have been limited to single-photon excitation. However, multiphoton-FRET *(22,23)* and single-particle FRET experiments *(24,25)* are finding their own place in biomedical applications in understanding biologically relevant interactions among the proteins such as conformation changes etc., at the atomic levels. With continual improvements in light sources, discovery of novel fluorophores and new detection devices, it is likely that FRET microscopy will emerge as an important biophysical tool in the biomedical sciences.

## 4. Notes

1. Forster distance $R_0$, is defined as that separation between the donor and acceptor, for which the energy transfer efficiency is 50% and is defined by the following expression:

$$R_0^6 = \left[8.75 \times 10^{-25} \times n^{-4} \times Q \times \kappa^2 \times J(\lambda)\right] \quad \text{(N.1)}$$

where $n$ is the refractive index of medium in the range of overlap, $Q$ is the quantum yield of the donor in the absence of acceptor, $J(\lambda)$ is the spectral overlap as shown in **Fig. 1B**. $\kappa^2$ is called the *orientation* factor, which depends on the angular orientation of the dipoles with respect to the vector separating them as well as with respect to each other (**Fig. 1A**) and is defined by

$$\kappa^2 = \left(\cos\theta_T - 3\cos\theta_A \times \cos\theta_D\right) \quad \text{(N.2)}$$

In general, this orientation factor can vary from 0 to 4, but is usually assumed to be 2/3, a value corresponding to a random orientation of the donors and acceptors. Typically, $R_0$ varies between 1 and 10 nm for various pairs of fluorophores (**Table 1**). The necessary criteria for the FRET pair (donor/acceptor) are summarized as follows: (i) The donor should be necessarily fluorescent with high quantum yield; (ii) acceptor excitation spectra ($A_A$)should have a substantial overlap with the donor emission spectra ($E_D$) but very little overlap with the donor excitation spectra ($A_D$); (iii) for a given donor–acceptor pair, the Forster distance is a constant in space and time. In order to measure a reasonable FRET signal, the donor–acceptor separation should be comparable to this value of $R_0$. For example, at $R = R_0$, the transfer efficiency is 50%, while this drastically reduces to 1.5% when $R = 2R_0$.

2. Energy transfer measured by all the FRET methods depends critically on the orientation factor that effectively represents an average angular profile of the fluorophores *(26)*. Because it is not directly measured, this can easily cause uncertainty in quantification of the FRET signals. On the other hand, it can be argued that a large hydrophobic FRET probe that is covalently bound to an amino acid chain of a protein is deprived of true rotational freedom. This would cause minimal uncertainty in orientation factor thereby making FRET quantification less ambiguous.
3. Equation 3 assumes that there is no acceptor fluorescence by direct excitation of the acceptor at the donor excitation wavelength. This is seldom realized in practice because of the spectral cross talk between the donor excitation and acceptor-excitation spectra. Regardless of these inherent problems, this method of observing FRET is the most common in wide-field fluorescence microscopes. One of the main drawbacks of this method is that both the donor and acceptor fluorescence can be quenched during excitation that will further make quantification difficult.
4. Analysis of the change in donor intensity before and after photobleaching of the acceptor is performed on a pixel-by-pixel basis to determine the FRET efficiency. An advantage of this method is that it requires only a single sample and that the energy transfer efficiency can be directly related to both the donor fluorescence and the acceptor fluorescence.
5. A practical way of calculating anisotropy in a typical fluorescence microscope experiment is by using a set of polarizers (for detecting light with parallel and perpendicular polarization) at the emission port of a microscope. Polarized excitation can be achieved either by having an excitation polarizer next to an arc lamp or using the polarized light output of a laser. A set of images is collected with two crossed polarizers (with respect to the excitation polarizer) at the emission port. The corresponding intensities for these two images ( for the entire cell or a selected region) are $I\|$ and $I \perp$, respectively. The anisotropy can be now calculated as

$$r = \frac{I_{\|} - I_{\perp}}{I_{\|} + 2I_{\perp}} \qquad \text{(N.3)}$$

An advantage of using this approach is that it is possible to observe FRET between two identical donor molecules (homo- or single-color FRET) and this eliminates the spectral cross-talk issues between the donor and acceptor. Fluorescein is one of the classical examples of homo-FRET with Forster distance approx 44 Å ***(10)***. Typical applications of this approach are in membrane organization issues, protein proximity measurements, and diffusion-limited kinetics. However, it is to be noted that not all fluorophores exhibit observable change in anisotropy.

6. Measuring FRET by FLIM methodology is a reliable way although it is usually commented that it lacks the sensitivity that is possible with any of the spectral methods. Temporal sensitivity of any FLIM system is decided primarily by the excitation pulse widths (in the case of time-domain methods) and the fast response of detectors. There are lasers available to provide ultrafast, femtosecond pulses (e.g., Titanium: Sapphire, Coherent Inc.) and fast CCD cameras (e.g., Argus HiSCA CCD cameras) are able to provide time resolutions as low as a few picoseconds. This combination can make the lifetime measurements equally sensitive for FRET measurements. Another relatively less explored methodology is spectral imaging microscopy, which combines the spectral resolution (around a few nanometers) of a spectrograph and spatial resolution (about a few hundred nanometers) of a microscope to give a wealth of information about nanoscale protein interactions in biological systems.
7. Filter selection is critical to the success of FRET imaging. For example a donor imaging pathway should be configured with an excitor filter that has bandwidth specific for the donor fluorophore and little or no excitation of the acceptor fluorophores. The dichroic and emission filters should be selected to eliminate as much of the acceptor emission as possible. The acceptor imaging pathway should be configured with an excitor filter of bandwidth that exclusively excites the acceptor fluorophore and with dichroic and emssion filters that block any emission from the donor molecule. The FRET imaging pathway must be configured with an excitor filter and dichroic filter that match those of the donor imaging pathway and an emission filter that matches that of the acceptor pathway.
8. CCD-cooled digital cameras are now available with high quantum efficiency over the spectrum from 200 to 1000 nm. Robust spectral response characteristics and special digital contrast enhancement circuits increase versatility for even the most difficult imaging conditions. Of late, electron-bombardment CCD cameras have come into use which employ an innovative high-gain sensor to obtain high-gain images in very low light.
9. If antibody labeling is to be accomplished, rinse the cells with appropriate buffer media (PBS or PHEM) to remove the debris and serum components from the cells. Choose the appropriate donor/acceptor antibody concentration (e.g., Cy3/Cy5-labeled antibodies or FITC/TRITC-labeled antibodies) for labeling. A preliminary binding affinity curve for each of the antibodies (donor/acceptor) has to be measured. For FRET experiments, usually a low, constant concentration of donor/acceptor (approx 50 μg/mL) antibody is employed and FRET efficiency is measured as the concentration of the acceptor is varied at a constant overall anti-

body (donor plus acceptor) concentration (typically donor/acceptor molar ratios in the range 1:1 to 1:5). It is necessary to ensure that the measured transfer efficiency is not biased due to concentration artifacts. Centrifuge donor/acceptor-labeled proteins/antibodies before use to remove large aggregates. Normal serum from the secondary antibody host is preferably used as a blocking reagent. Alternately, one can use 0.5% bovine serum albumin (BSA) in PBS for blocking nonspecific binding of the antibodies. Prepare labeling mixtures (antibody + blocking reagent) in a buffer medium at physiological pH (approx 7.2). If cytoplasmic labeling has to be accomplished, then the membrane has to be permeabilized to allow antibodies into the cell. In fixed cells, either precipitation by anhydrous 100% methanol (–20 to 10°C ) or cross-linking/permeabilization by 4% paraformaldehyde (37°C) and 0.1% Triton X-100 (4°C) can be used. In living cells, microinjection, transient hypoosmotic shock, ATP permeabilization, or other methods can be utilized.

10. Sealant should not contain acetone or other denaturants that might denature the fluorescent protein, thus destroying its ability to fluoresce.
11. When using a confocal laser scanning microscope, the same principle applies, the imaging pathway for the FRET sample must be a hybrid consisting of excitation pathway matched to the donor excitation pathway and the emission pathway matched to that of the acceptor. For example, the three imaging pathways used in a Zeiss 510 laser scanning confocal microscope are as represented in **Fig. 3A**. The acceptor-only signal is excited with the 514 nm line and collected in PMT 1, the donor-only signal is excited with the 458 nm and collected in PMT 2, and the FRET signal is excited by 458 nm and collected in PMT 1. The signals are collected in sequence using the "multitracking" configuration to minimize the cross-talk. Optics with both chromatic and spherical corrections will likely not have the most efficient transmission characteristics and therefore signal will be reduced. However, these corrections are important to ensure that excitation and emission are occurring in the same focal plane. This is particularly important when using a laser scanning confocal for FRET acquisition.
12. The various filters in a FRET set are chosen to minimize any potential cross talk between signals, although even with optimal selection of filters, this still remains a problem. A 12-bit confocal image would be optimized to a maximum of approx 3275 intensity units. This is repeated for the acceptor sample and acceptor filter set, and the FRET sample with the FRET filter set. Once the acquisition settings are determined for a filter set, they must not be altered regardless of the sample being acquired. Computer macros or journals may be written to "automate" acquisition once the initial parameters are established. While the fluorescence filters and neutral-density filters can be changed manually, it is far more time efficient to have motorized filter wheels that can be driven by the acquisition software such as is possible with Metamorph (Universal Imaging Corp., Downington, PA). Alternatively, confocal data sets may be acquired using "multitracking" (Zeiss LSM 510) or sequential imaging (Olympus FV500) that are existing functions of the operating software.

13. It is important to have precise intensity analysis to rule out noise contributions from autofluorescence, spectral cross-talk, and so on. Furthermore the effects of quenching or irreversible photobleaching have to be taken into account. In addition, usually the orientation factor is assumed to be 2/3 that is the average of a randomized ensemble of donor/acceptor dipoles. A few seminal works on FRET quantification take into account all the above features so as to give a reliable estimate of FRET efficiency in practice *(21,27,28)*.

## Acknowledgments

We gratefully acknowledge Yingpei Zhang, Marisa Lopez-Cruzan, and Eva Biener for their useful suggestions in this manuscript and Atsushi Masuda for providing us with the BHK specimens.

## References

1. Pawley, J. B. (1995) *Handbook of Biological Confocal Microscopy*. Plenum Press, New York, NY.
2. Dyba, M. and Hell, S. W (2002) Focal spots of size λ/23 open up far-field fluorescence microscopy beyond 33 nm axial resolution. *Phys. Rev. Lett.* **88,** 163,901–163,904.
3. Herman, B. (1989) Resonance energy transfer microscopy. *Meth. Cell Biol.* **30,** 219–243.
4. Wu, P. G. and Brand, L. (1994) Resonance energy transfer: methods and applications. *Anal. Biochem. 218,* ***1–13.***
5. Clegg, R. M. (1995) Fluorescence resonance energy transfer. *Curr. Opin. Biotechnol.* **6,** 103–110.
6. Selvin, P. R. (2000) The renaissance of fluorescence resonance energy transfer. *Nat. Struct. Biol.* **7,** 730–734.
7. Lakowicz, J. R. (1999) *Principles of Fluorescence Spectroscopy*, 2nd Ed. Plenum, New York, NY.
8. Stryer, L. and Haughland, R. P. (1967) Energy transfer: a spectroscopic ruler. *Proc. Natl. Acad. Sci. USA* **58,** 719–726.
9. Jovin, T. M. and Jovin, D. J. A. (1989) FRET microscopy: Digital imaging of fluorescence resonance energy transfer. Application in cell biology, in *Cell Structure and Function by Microspectrofluorometry* (Kohen, E. and Hirschberg, J. G., eds.). Academic, San Diego, CA, pp. 99–116.
10. Krishnan, R. V, Varma, R., and Mayor, S (2001) Fluorescence methods to probe nanometer scale organization of molecules in living cell membrane. *J. Fluorescence* **11,** 211–226.
11. Weber, G. (1954) Dependence of the polarization of the fluorescence on concentration. *Trans. Faraday Soc.* **50,** 552–555.
12. Runnels, L. W. and Scarlata, S. F. ( 1995) Theory and application of fluorescence homotransfer to melitin oligomerization. *Biophys. J.* **69,** 1569–1583
13. Varma, R. and Mayor, S. (1998), GPI-anchored proteins are organized in submicron domains at the cell surface. *Nature* **394,** 798–801.

**14.** Gautier, I., Tramier, M., Durieux, C., et al. (2001) Homo-FRET microscopy in living cells to measure monomer-dimer transition of GFP-tagged proteins. *Biophys. J.* **80,** 3000–3008.
15. Bastiaens, P. I. H. and Squire, A. (1999) Fluorescence lifetime imaging microscopy: spatial resolution of biochemical processes in the cell. *Trends. Cell. Biol.* **9,** 48–52
16. Pepperkok, R., Squire, A., Geley, S., and Bastiaens, P. I. H. (1999) Simultaneous detection of multiple green fluorescent proteins in live cells by fluorescence lifetime imaging microscopy. *Curr. Biol.* **9,** 269–272.
17. Wang, X. F., Periasamy, A., Wodnicki, P., Gordon, G. W., and Herman, B. (1996) Time-resolved fluorescence lifetime imaging microscopy: instrumentation and biomedical applications in *Fluorescence Imaging spectroscopy and Microscopy* (Wang, X. F. and Herman, B., eds.) JohnWiley, New York, NY, pp. 313–350.
18. www.universal-imaging.com; www.qimaging.com; www.intelligent-imaging.com.
19. Tsien, R. Y. (1998) The green fluorescent protein. *Annu. Rev. Biochem.* **67,** 509–544, and references therein.
20. Hicks, B. W. (ed.) (2002) *Green Fluorescent Protein*. Humana, Totowa, NJ.
21. Gordon, G. W., Berry, G., Liang, X. H., Levine, B., and Herman, B. (1998) Quantitative fluorescence resonance energy transfer measurements using fluorescence microscopy. *Biophys. J.* **74,** 2702–2713.
22. Konig, K. (2000) Multiphoton microscopy in life sciences. *J. Microsc.* **200,** 83–104
23. Majoul, I., Straub, M., Duden, R., Hell, S. W., and Soling, H. D. (2002) Fluorescence resonance energy transfer analysis of protein–protein interactions in single living cells by multifocal multiphoton microscopy. *Rev. Mol. Biotechnol.* **82,** 267–277.
24. Ha, T., Enderle, T. H., Ogletree, D. F., Chemla, D. S., Selvin, P. R., and Weiss, S. (1996) Probing the interaction between two single molecules: fluorescence resonance energy transfer between single donor and a single acceptor. *Proc. Natl. Acad. Sci. USA* **93,** 6264–6268.
25. Ha, T., Ting, A. Y., Liang, J., et al. (1999) Temporal fluctuations of fluorescence resonance energy transfer between two dyes conjugated to a single protein. *Chem. Phys.* **247,** 107–118.
26. Dale, R. E., Eisinger, J., and Blumberg, W. E. (1979) The orientational freedom of molecular probes. The orientation factor in intramolecular energy transfer. *Biophys. J.* **26,** 161–193.
27. Nagy, P., Vamosi, G., Bodnar, A., Lockett,S. J., and Szollosi, J. (1998) Intensity-based energy transfer measurements in digital imaging microscopy. *Eur. Biophys. J.* **27,** 377–389
28. Xia, Z. and Liu, Y. (2001) Reliable and global measurement of fluorescence resonance energy transfer using fluorescence microscopes. *Biophys. J.* **81,** 2395–2402.